Available online at www.sciencedirect.com
SCIENCE DIRECT®
International Journal of Pharmaceutics 257 (2003) 169–180
international journal of pharmaceutics
www.elsevier.com/locate/ijpharm

Optimization of the preparation process for human serum albumin (HSA) nanoparticles

K. Langer [a,*], S. Balthasar [a], V. Vogel [b], N. Dinauer [c], H. von Briesen [c], D. Schubert [b]

[a] *Institut für Pharmazeutische Technologie, Biozentrum Niederursel, Johann Wolfgang Goethe-Universität, Marie-Curie-Straße 9, Frankfurt am Main D-60439, Germany*
[b] *Institut für Biophysik, Johann Wolfgang Goethe-Universität, Theodor-Stern-Kai 7, Frankfurt am Main D-60590, Germany*
[c] *Georg-Speyer-Haus, Institute of Biomedical Research, Paul-Ehrlich-Straße 42-44, Frankfurt am Main D-60552, Germany*

Received 18 September 2002; received in revised form 9 January 2003; accepted 7 February 2003

Abstract

Nanoparticles prepared by desolvation and subsequent crosslinking of human serum albumin (HSA) represent promising carriers for drug delivery. Particle size is a crucial parameter, in particular for the in vivo behaviour of nanoparticles after intravenous injection. The objective of the present study is the development of a desolvation procedure for the preparation of HSA-based nanoparticles under the aspect of a controllable particle size between 100 and 300 nm in combination with a narrow size distribution. A pump-controlled preparation method was established which enabled particle preparation under defined conditions. Several factors of the preparation process, such as the rate of addition of the desolvating agent, the pH value and the ionic composition of the HSA solution, the protein concentration, and the conditions of particle purification were evaluated. The pH value of the HSA solution prior to the desolvation procedure was identified as the major factor determining particle size. Varying this parameter, (mean) particle diameters could be adjusted between 150 and 280 nm, higher pH values leading to smaller nanoparticles. Washing the particles by differential centrifugation led to significantly narrower size distributions. The reproducibility of the particle size and particle size distribution under the proposed preparation conditions was demonstrated by sedimentation velocity analysis in the analytical ultracentrifuge and the cellular uptake of those nanoparticles was studied by confocal microscope imaging and FACS analysis. The stability of the resulting nanoparticles was evaluated by pH and buffer titration experiments. Only pH values distinctly outside the isoelectric pH range of HSA and low salt concentrations were able to prevent nanoparticle agglomeration.

Keywords: Nanoparticles; Human serum albumin (HSA); Particle size distribution; Cellular uptake

1. Introduction

The body distribution of colloidal drug carrier systems is mainly influenced by two physicochemical properties, particle size and surface characteristics (Moghimi et al., 2001). Concerning particle size, the particles should be small enough not to be removed by simple filtration mechanisms in a capillary bed after intravenous injection. With respect to the surface characteristics of a colloidal system, these characteristics may directly affect particle size. Above all, however, they represent the major determinant for

* Corresponding author. Tel.: +49-69-798-29692; fax: +49-69-798-29694.
E-mail address: k.langer@em.uni-frankfurt.de (K. Langer).

0378-5173/03/$ – see front matter
doi:10.1016/S0378-5173(03)00134-0

protein adsorption in biological fluids and may modify particle interaction with specific plasma membrane receptors, thus leading to elimination of the particles from the systemic circulation. The mechanism of protein adsorption on particle surfaces in conjunction with the recognition of such coated particles by monocytes and macrophages is named opsonization process. This opsonization process seems to be influenced by the surface curvature of the carrier system, smaller carriers leading to a reduced adsorption of proteins and opsonins and in turn to a reduced uptake of such systems by phagocytic cells (Harashima et al., 1994). It was observed that the extent of opsonization decreased with a decrease in particle size from 800 to 200 nm, and no enhancement of phagocytic uptake due to opsonization was recorded at particle sizes below 200 nm. For very small colloidal systems, with a size below 100 nm, it was described that after intravenous injection these carriers were able to cross the fenestration in the hepatic sinusoidal endothelium, leading to a hepatic accumulation instead of long intravasal circulation. Even systems such as liposomes, with a size range of about 400 nm and a highly deformable structure, were able to cross the endothelial fenestration, whereas rigid systems of the same diameter did not (Romero et al., 1999). Since nanoparticles are characterized by a solid particle matrix, according to the findings described a long-circulating system can only be achieved in a size range between 100 and 200 nm in diameter. As a consequence, a major aspect in preparing a colloidal drug carrier system has to be establishing preparation conditions which control the resulting particle size and which lead to particles of a narrow size distribution, with special emphasis on sizes of 100–200 nm.

Among the available potential colloidal drug carrier systems covering the size range described, protein-based nanoparticles play an important role. Basically three different methods for their preparation have been described, based on emulsion formation, desolvation, or coacervation. Most often serum albumin of different origin as well as gelatin were used as the starting material for the preparations. With respect to emulsion techniques applying human serum albumin (HSA), a complete and systematic study concerning the influence of protein concentration, emulsification time and power, stirring rate, heat stabilization temperature, and the type of the non-aqueous phase was carried out by Gallo et al. (1984). A method for the preparation of bovine serum albumin nanoparticles in the sub-200-nm range was described by Müller et al. (1996). The disadvantage of the emulsion methods for particle preparation is the need for applying organic solvents, for the removal both of the oily residues of the preparation process and of surfactants required for emulsion stabilization. Therefore, as an alternative method for the preparation of nanoparticles a desolvation process derived from the coacervation method of microencapsulation was developed. In 1993, Lin et al. described the preparation of HSA nanoparticles of diameter around 100 nm using a surfactant-free pH-coacervation method (Lin et al., 1993). The particles were prepared by the dropwise addition of acetone to an aqueous HSA solution at pH values between 7 and 9, followed by glutaraldehyde crosslinking and purification by gel permeation chromatography. It was found that with increasing pH value of the HSA solution particle size was reduced, apparently due to an increased ionization of the HSA (isoelectric point pI = 5.3) which leads to repulsion of the HSA molecules and aggregates during particle formation. HSA nanoparticles were obtained in a size range between 90 and 250 nm, by adjusting the pH and by controlling the amount of added acetone. The described nanoparticles were of spherical shape, but TEM revealed a broad size distribution. No further data concerning the polydispersity of the nanoparticles prepared under different conditions was given. A major shortcoming of the paper is that pH was adjusted in the absence of salt, whereas it is well-known that, under these conditions, pH measurements applying glass electrodes (as usually done) are of limited reliability, in particular in the presence of high concentrations of protein (Westcott, 1978).

The objective of the present study is the optimization of a desolvation procedure for the preparation of HSA-based nanoparticles which show a controllable particle diameter between 100 and 300 nm and a narrow size distribution. In addition, we have studied the cellular uptake of these nanoparticles by confocal microscope imaging and FACS analysis. Together with our previous work on the covalent surface modification of such nanoparticles (Langer et al., 2000; Weber et al., 2000a) the study is intended to establish a rational basis for the production and

application of protein-based nanoparticles as drug carrier systems.

2. Materials and methods

2.1. Reagents and chemicals

HSA (fraction V, purity 96–99%) and glutaraldehyde, 8% solution, were obtained from Sigma (Steinheim, Germany). All other reagents were purchased from Merck (Darmstadt, Germany); they were of analytical grade and used as received.

2.2. Preparation of HSA nanoparticles

HSA nanoparticles were prepared by a desolvation technique as described previously (Marty et al., 1978; Weber et al., 2000b). In principle, between 50 and 200 mg HSA in 2.0 ml of purified water or 10 mM NaCl solution, respectively, both titrated to pH 7–10, were transformed into nanoparticles by the continuous addition of 8.0 ml of the desolvating agent ethanol under stirring (500 rpm) at room temperature. The technique was modified by adding a tubing pump (Ismatec IPN, Glattbrugg, Switzerland) which enabled nanoparticle preparation at a defined rate of ethanol addition between 0.5 and 2.0 ml/min. After the desolvation process, 8% glutaraldehyde in water (between 0.235 and 1.175 μl/mg HSA) was added to induce particle crosslinking. The crosslinking process was performed under stirring of the suspension over a time period of 24 h.

2.3. Purification of HSA nanoparticles

The resulting nanoparticles were purified by five cycles of differential centrifugation (20,000 × *g*, 8 min) and redispersion of the pellet to the original volume in water or 10 mM NaCl at pH values of 7 and 9, respectively. Each redispersion step was performed in an ultrasonication bath (Elma Transsonic Digital T790/H) over 5 min.

2.4. Determination of particle size and size distribution

Average particle size was measured by photon correlation spectroscopy (PCS) using a Malvern zetasizer 3000HSA (Malvern Instruments Ltd., Malvern, UK). The samples were diluted 1:400 with purified water and measured at a temperature of 25 °C and a scattering angle of 90°. In parallel, in part of the samples the size distribution was studied by sedimentation velocity analysis in the analytical ultracentrifuge (Vogel et al., 2002), making use of the superior resolving power of this technique (Schuck, 2000; Schuck and Rossmanith, 2000; Schuck et al., 2002). In principle, the nanoparticle stock solution was brought, by addition of appropriate concentrated solutions and water, to 20 mM sodium phosphate (pH 7), 150 mM NaCl, 23.5% (w/v) sucrose, at a solute concentration giving a turbidity between 0.6 and 0.7 at 420 nm in a cuvette with a 1 cm optical pathlength. Unpurified nanoparticle samples in addition contained approximately 10% ethanol. The ultracentrifugal experiments were performed using a Beckman Optima XL-A ultracentrifuge at rotor speeds of 3000 or 5000 rpm as described earlier (Vogel et al., 2002). The apparent absorbance (turbidity) versus radius data (collected at 420 nm) were modeled as a distribution of non-diffusing spherical particles, based on the results described (Vogel et al., 2002). The calculations used the *ls−g**(*s*)-variant of the *sedfit* program by Schuck (Schuck and Rossmanith, 2000; Schuck et al., 2002).

2.5. Determination of the non-desolvated HSA after desolvation

For the determination of the percentage of non-desolvated HSA, the nanoparticles were separated from the supernatant by centrifugation at 16,000 × *g* for 20 min at room temperature. An aliquot of the supernatant (100.0 μl) was diluted with 900.0 μl water and the amount of the dissolved HSA in the supernatant was determined using a standard BCA protein assay (Smith et al., 1985). To 50.0 μl of the supernatant, 1000.0 μl of the BCA working reagent were added. After incubating the mixture at 37 °C for 30 min, the samples were analyzed spectrophotometrically at 562 nm. The protein content of the samples, as well as that of the starting HSA solution, was calculated relative to reference samples, which contained different volumes of a HSA standard solution and were treated as described before.

2.6. Determination of pH-dependent particle size and zetapotential

Titration experiments on the HSA nanoparticles were performed over a pH range between 3 and 10 using the Malvern zetasizer 3000HSA together with an autotitrator MPT-1 (Malvern Instruments Ltd.). For the analysis, 100 μl of nanoparticle suspension were diluted with 50 ml purified water and the pH value of the suspension was automatically adjusted by the titration unit by addition of 0.1N hydrochloric acid or 0.1N sodium hydroxide solution, respectively. At 8 predefined pH values between 3 and 10, the zetapotential of the nanoparticles was measured by microelectrophoresis and the particle size was determined by PCS (in two separate flow cells).

2.7. Determination of the salt dependency of surface charge

The salt dependency of the surface charge was determined as described for the corresponding pH dependent parameter, except that the autotitration experiment was performed by the addition of a 10-fold concentrated phosphate buffer (pH 7.4). At 8 predefined buffer concentrations between 0 and 230 mM, the zetapotential of the nanoparticles was measured by microelectrophoresis in a flow cell.

2.8. Cellular uptake of HSA nanoparticles

Peripheral blood mononuclear cells (PBMC) were separated from buffy coats of healthy HIV-1 seronegative male donors by density gradient centrifugation over Ficoll-Hypaque. For generation of monocyte-derived macrophages the separated PBMC were cultured on hydrophobic Teflon foils (Biofolie 25; Heraeus, Hanau, Germany) for 7 days at a cell density of 3.3×10^6 cells/ml in RPMI 1640 (Biochrom, Berlin, Germany) supplemented with antibiotics (100 U/ml penicillin and 100 mg/ml streptomycin; Gibco, Berlin, Germany), L-glutamine (2 mM; Gibco), and 4% pooled human AB-group serum. After the indicated time period cells were harvested and washed twice with RPMI 1640. Viable cells were counted by trypan blue exclusion. Monocyte derived macrophages (4.5×10^5 cells) were plated on chamber slides (NUNC GmbH, Wiesbaden, Germany). After 1 h nonadherent cells were removed by repeated washing and cells were cultured with fresh medium. On the following day HSA nanoparticles were added at a final concentration of 25 μg/ml and incubated for 3 h with the cells.

For confocal microscope imaging cells were washed with PBS and subsequently fixed in methanol for 6 min at −20 °C. Cell nuclei were stained with TOTO-3-iodid (Molecular Probes Europe BV, Leiden, The Netherlands) and cell membranes were stained with tetramethylrhodamine-isothiocyanat (TRITC)-conjugated concanavalin A. Finally cells were embedded in a mixture of 10% Mowiol 488™, 2.5% diazabicyclooctan (DABCO) and 25% glycerol in 0.2 M TRIS buffer pH 8.5. Pictures were taken using a confocal microscope Leica DM IRBE (Leica Mikrosysteme GmbH, Bensheim, Germany).

For quantification of cellular uptake by FACS analysis cells were washed twice with PBS and subsequently fixed in CellFix solution (Becton Dickinson, San Jose, USA). FACS was performed with 10,000 cells per condition, using FACSCalibur and CellQuest Pro software (Becton Dickinson, San Jose, USA).

3. Results and discussion

The objective of the present study was to optimize the preparation procedure for HSA nanoparticles with respect to a defined particle size and particle size distribution and to study their cellular uptake. The study is based on our earlier work (Weber et al., 2000b) describing a desolvation method for HSA particle preparation and their characterization with respect to size, zetapotential and the number of available amino groups on their surface. In the earlier study, the amount of the desolvating agent ethanol in the desolvation process was found to control particle size, but the variability in size at a given ethanol amount was high. In part this variability probably can be attributed to the manual performance of the desolvation process, characterized by a drop by drop addition of the desolvating agent. In the present study, the manual desolvation procedure was, therefore, replaced by a pump-controlled system which enabled nanoparticle preparation at a defined rate of ethanol addition (between 0.5 and 2.0 ml/min). Furthermore, additional parameters such as the composition and the pH value of the HSA

solution prior to the desolvation procedure and the purification of the nanoparticles were optimized in order to achieve a colloidal system with well-defined physicochemical characteristics. Such a system is a prerequisite if surface modification procedures aiming at specific drug binding and targeting properties are to be applied (Langer et al., 2000; Weber et al., 2000a).

3.1. Nanoparticle formation: optimization of the desolvation step; average particle size

In order to influence the resulting particle size, the rate of ethanol addition during the desolvation procedure as well as the pH value of the protein solution used for desolvation was varied. In a first set of experiments performed at pH 7, the rate of ethanol addition showed no significant influence on the average diameter of the resulting nanoparticles, which was around 280 nm (Fig. 1). According to PCS data, the rate of ethanol addition mainly influenced the width of the particle size distribution: At a rate of 0.5 ml/min, nanoparticles with a polydispersity index of about 0.10 were obtained, whereas a rate between 1.0 and 2.0 ml/min led to nanoparticles with a more uniform size characterized by polydispersity indices in the range between 0.01 and 0.02. Using the standard BCA protein assay, a particle yield of about 95% was determined over the whole rate range of ethanol addition (data not shown). As a consequence of the results described, the subsequent experiments were performed with the pump-controlled system set at a rate of ethanol addition of 1.0 ml/min.

In contrast to the lack of influence of the rate of ethanol addition, the pH value of the HSA solution prior to ethanol addition strongly influenced the resulting particle size (Fig. 2). At pH > 7 particle diameter was significantly reduced with increasing pH value to finally about 150 nm at pH > 9. In addition, also the particle yield significantly decreased with increasing pH, from about 95% at pH 7 to 66% at pH 9. Both observations are in good agreement with the earlier work of Lin et al. (1993) who used a slightly different surfactant-free pH-coacervation method in which albumin desolvation was achieved by the addition of acetone.

As it is difficult to adjust the correct pH value in the absence of salt and in the presence of high concentrations of protein (Westcott, 1978), several attempts were undertaken to establish a HSA desolvation method under buffered conditions. Phosphate buffer (pH 7 and 8) USP, and alkaline borate buffer (pH 8 and 9) USP were used in concentrations between 20 and 50 mM. HEPES buffer (pH 7.5) and TRIS buffer (pH 8 and 9) were under evaluation in concentrations between 20 and 200 mM. All of the buffer salts applied

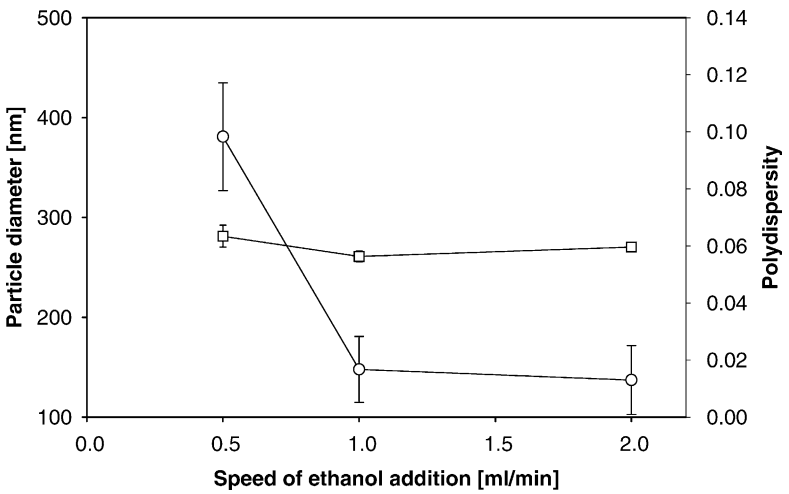

Fig. 1. Diameter (□) and polydispersity index (○) of HSA nanoparticles prepared in water at pH 7 as a function of the rate of ethanol addition (mean ± S.D.; $n \geq 3$). Initial HSA concentration: 100 mg/ml.

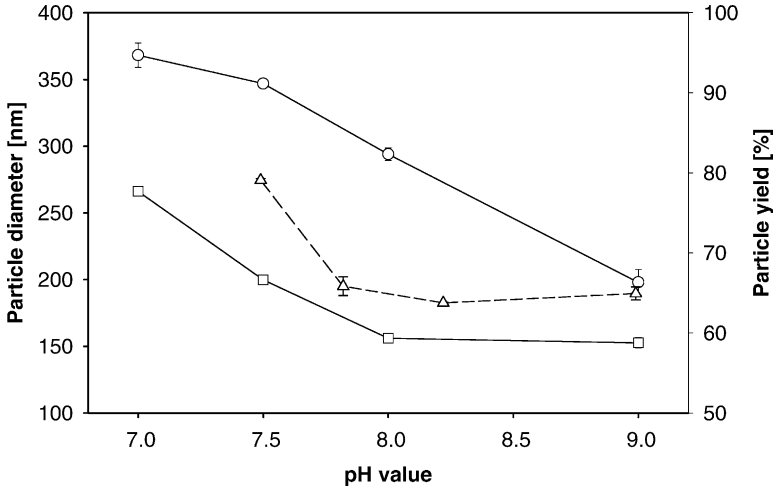

Fig. 2. Influence of the pH value on the diameter (□) and yield (○) of HSA nanoparticles prepared in pure water and on the diameter of HSA nanoparticles prepared in 10 mM NaCl solution (△) (mean ± S.D.; $n = 3$). Rate of ethanol addition: 1.0 ml/min; initial HSA concentration: 100 mg/ml.

interfered either with the desolvation process, leading to large HSA aggregates or precipitation of the buffer salts, or with the crosslinking process of the nanoparticles. With phosphate buffer, salt precipitation occurred during the desolvation procedure, whereas the alkaline borate buffer as well as the HEPES buffer led to a precipitation of the HSA in large agglomerates instead of the formation of nanoparticles. In the presence of TRIS buffer, nanoparticles were obtained but due to their primary amino group the TRIS molecules interfered with the glutaraldehyde crosslinking of the particle matrix. We have, therefore, abandoned the use of buffers but have performed the nanoparticle preparation in the presence of 10 mM NaCl as ionic background for the adjustment of pH (Westcott, 1978). Again, average particle diameters decreased with increasing pH of the HSA solution, starting with around 275 nm at pH 7.5 and being lowered to 180 nm at pH 9 (Fig. 2). In contrast to a preparation in pure water no reproducible particle formation could be achieved at pH values below 7.5. In the presence of sodium chloride average particle diameter could thus be controlled by proper choice of the pH of particle formation. In general, at the same nominal pH it was somewhat larger than with the nanoparticles assembled in pure water, probably due to the shielding of surface charges by the added ions and thus to reduced repulsion between the macromolecular components.

The influence of the HSA concentration on particle diameter and polydispersity of the resulting samples, at pH 8.2 and in the presence of 10 mM NaCl, is shown in Fig. 3. In a HSA concentration range between 25 and 100 mg/ml only a slight influence on the particle diameter was observed, with a shallow size minimum of 155 nm at 50 mg/ml HSA. With increasing HSA concentration the polydispersity of the samples was somewhat reduced (Fig. 3).

3.2. Particle purification and resulting size distributions

The characterization of the assembled HSA nanoparticles described up to now were performed on particles that had undergone the final purification procedure (repeated differential centrifugation) in pure water without pH adjustment. The effect of the procedure as well as possible improvements were studied by determining the size and size distribution of differently treated nanoparticles by sedimentation velocity analysis in the analytical ultracentrifuge. Results obtained with one unpurified sample and three samples obtained from it by washing procedures differing slightly from each other are shown in Fig. 4A. Obvi-

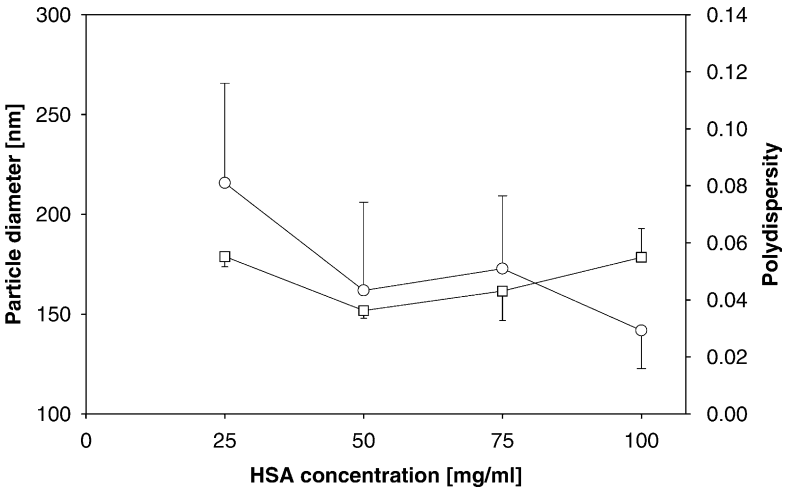

Fig. 3. Diameter (□) and polydispersity index (○) of HSA nanoparticles prepared at different HSA concentrations in the presence of 10 mM NaCl at pH 8.2 (mean ± S.D.; $n = 3$). Rate of ethanol addition: 1.0 ml/min.

ously, the washing removes from the sample virtually all particles of diameter below around 70 nm, which leads to much narrower size distributions. The actual degree of purification is even much greater than indicated by the figure since, at the rotor speeds used, uncomplexed HSA and small complexes virtually do not sediment and thus do not show up in the analysis (in addition, due to their low specific turbidity their contribution to the overall signal is very small in any case). Varying the pH of the washing solution or bringing it to 10 mM NaCl, on the other hand, had little or no influence on the size distributions, in contrast to the effect of these parameters during particle formation. In order to avoid possible particle aggregation in those cases where the pH of the solution may have dropped (due to dissolved CO_2) to values close to the p*I* of HSA (see below), we have introduced into the standard procedure washing at pH 9. The purification procedure described is to be preferred to that used by Lin et al., gel filtration (Lin et al., 1993), since it is more readily applied to much larger sample volumes.

Considering the results on the influence of the different parameters under evaluation, a standard protocol for the preparation of HSA nanoparticles was established. According to this protocol the nanoparticles were prepared in 10 mM NaCl, at a starting HSA concentration of 100 mg/ml. The pH of this solution was adjusted to 8.2. Nanoparticles were assembled at a rate of ethanol addition of 1.0 ml/min, which grants a low polydispersity index (Fig. 1). Together these conditions lead to particles with average diameters below 200 nm (Fig. 2), at a particle yield of about 75% (Fig. 2). The crosslinked nanoparticles were purified under alkaline washing conditions (pH 9) in order to separate smaller particles and to achieve a narrow particle size distribution.

To test the reproducibility of particle preparation, three different preparations of HSA nanoparticles, assembled under the standard conditions just described, were analyzed by sedimentation velocity analysis in the analytical ultracentrifuge. The results are shown in Fig. 4B. It is obvious from the figure that the preparation method applying a pump-controlled system in combination with a defined pH adjustment in the presence of sodium chloride, as introduced by us, leads to well-defined mean particle sizes as well as to narrow particle size distributions. These distributions, now containing only particles with diameters exceeding approximately 70 nm, can be further fractionated by preparative sucrose gradient centrifugation (Vogel et al., 2002).

3.3. Stability and surface charge of the nanoparticles

The stability and electrical behaviour of the HSA nanoparticles were evaluated by pH and buffer titration

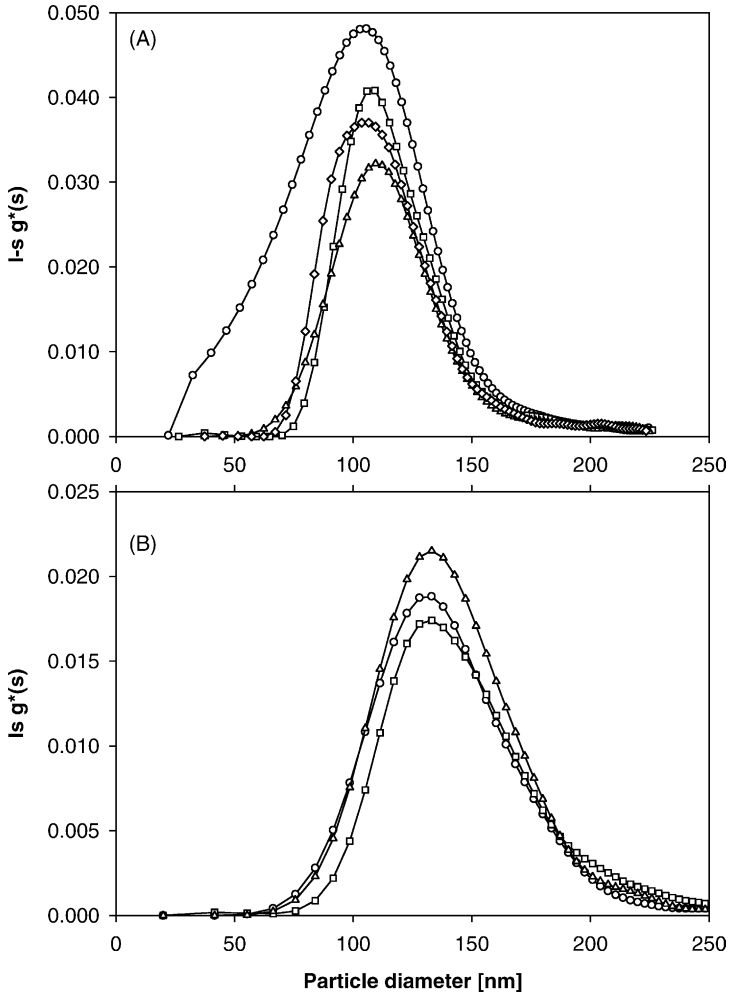

Fig. 4. Size distribution of HSA nanoparticles according to sedimentation velocity analysis: (A) After formation and crosslinking the nanoparticles were treated under different conditions: no washing (○), washing with water (no pH adjustment) (□), washing with water adjusted to pH 9 (△), and with 10 mM NaCl pH 9 (◇). (B) Three independent samples of HSA nanoparticles were prepared under identical conditions in 10 mM NaCl at pH 8.2. The nanoparticles were purified under alkaline washing conditions. For the rate of ethanol addition and HSA concentration see Fig. 2.

experiments. A typical titration profile of preformed nanoparticles over a pH range between 3 and 10 is outlined in Fig. 5. The titration was started at pH 3. Under these conditions the nanoparticles revealed a particle diameter of about 250 nm and a zetapotential of +38 mV. With increasing pH value the zetapotential of the nanoparticles was reduced to −40 to −50 mV at pH values between 7.2 and 10. The isoelectric point (p*I*) of the HSA nanoparticles was calculated to be 5.05 (i.e. 0.25 pH units lower than for unmodified HSA). At pH values around the p*I*, the nanoparticles became unstable, as indicated by PCS: particle diameter increased from 250 nm to about 2.7 μm. The particle aggregation was largely irreversible even at higher pH values at which the nanoparticles exhibited a pronounced surface charge. Although a reduction of the particle diameter from 2.7 μm to about 700 nm was observed due to the negative surface charge at these pH values, the initial size of 250 nm was not reached. Therefore, when handling protein-based

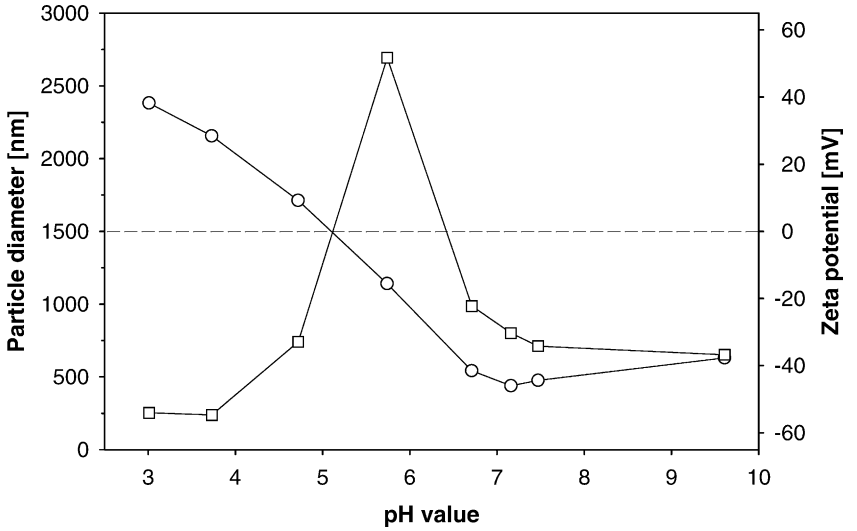

Fig. 5. Influence of the pH value on the diameter (□) and zetapotential (○) of preformed HSA nanoparticles. For other experimental parameters see Fig. 2.

nanoparticles, pH values leading to neutral particle surface charges have to be avoided. This observation is of major importance for further surface modification steps by protein chemistry which require a pH adjustment of the reaction media.

In order to take a detailed look at the effect of crosslinking on the p*I* of HSA nanoparticles, the particles were prepared with different amounts of the crosslinker glutaraldehyde. Thus, after the desolvation procedure the nanoparticles were crosslinked, per milligram HSA, with 0.235, 0.588 or 1.175 μl of an aqueous 8% glutaraldehyde solution. These glutaraldehyde concentrations equal 40, 100 and 200% of the calculated amount necessary for the quantitative crosslinking of the 59 ε-amino groups of lysine in the HSA molecules of the particle matrix (Hirayama et al., 1990; Carter and Ho, 1994). Whereas no influence of the crosslinking conditions on the resulting

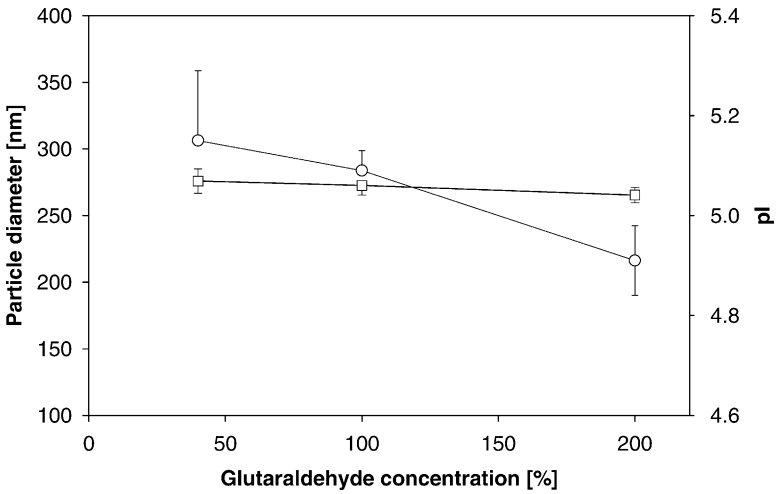

Fig. 6. Influence of the crosslinking process with different amounts of glutaraldehyde on the diameter (□) and p*I* (○) of the resulting HSA nanoparticles (mean ± S.D., $n = 3$). For other experimental parameters see Fig. 2.

particle size was observed (Fig. 6), the glutaraldehyde crosslinking of the particle matrix tends to result in a decrease in the p*I* of the nanoparticles ($P = 0.057$, Student's *t*-test): the p*I* value decreased from 5.3 (without crosslinker) to 5.15 (40% crosslinker), 5.09 (100% crosslinker) and 4.91 (200% crosslinker), respectively. Such reduction in the p*I* value could be expected for a covalent reaction involving lysine side chains of a protein.

The salt dependency of the surface charge of preformed HSA nanoparticles was determined by a titration experiment in which increasing amounts of a 1130 mM phosphate buffer (pH 7.4) were added to the aqueous nanoparticle suspension. With increasing buffer concentration the zetapotential of the nanoparticles was reduced from about −60 mV without buffer to −20 mV under isotonic conditions (Fig. 7), due to a shielding of the surface charge of the nanoparticles by the ionic species of the buffer. Nevertheless, it is obvious that phosphate buffer of pH 7.4 can be used at least up to concentrations of 150 mM without reducing particle surface charge to a degree that leads to isoelectric aggregation of the particles.

3.4. Cellular uptake of HSA nanoparticles

In order to investigate the potential of HSA nanoparticles to serve as a colloidal drug carrier cellular uptake studies were performed with primary human blood-derived macrophages. HSA nanoparticles were prepared and characterized as described in Section 2 showing an average diameter of 187.6 nm and a zetapotential of −44 mV. After an incubation time of 3 h a remarkable intracellular accumulation of HSA nanoparticles was observed using confocal microscope imaging (Fig. 8A). At a concentration of 25 μg/ml autofluorescent HSA nanoparticles were mostly distributed within non-nucleic intracellular compartments (Fig. 8B). Quantification of cellular uptake by FACS analysis shows a concentration-dependent accumulation of HSA nanoparticles in primary human blood-derived macrophages. As seen in Fig. 9 at a concentration of 25 μg/ml about 87% of the cells have taken up HSA nanoparticles. Above a concentration of 100 μg/ml nearly all cells have internalized HSA nanoparticles.

These findings indicate that HSA nanoparticles prepared by the desolvation technique with small average

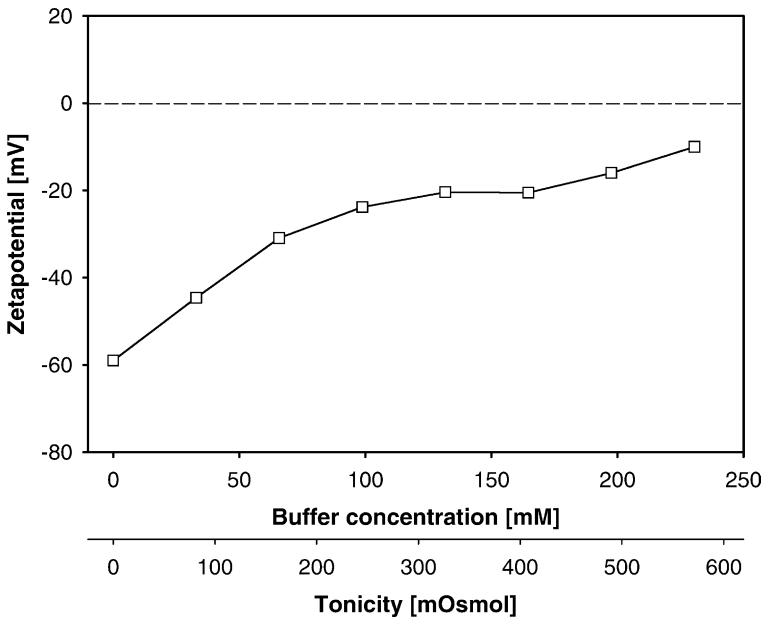

Fig. 7. Influence of the phosphate buffer concentration (pH 7.4) on the zetapotential of preformed HSA nanoparticles. The corresponding tonicity of the nanoparticle suspension is given as a second axis.

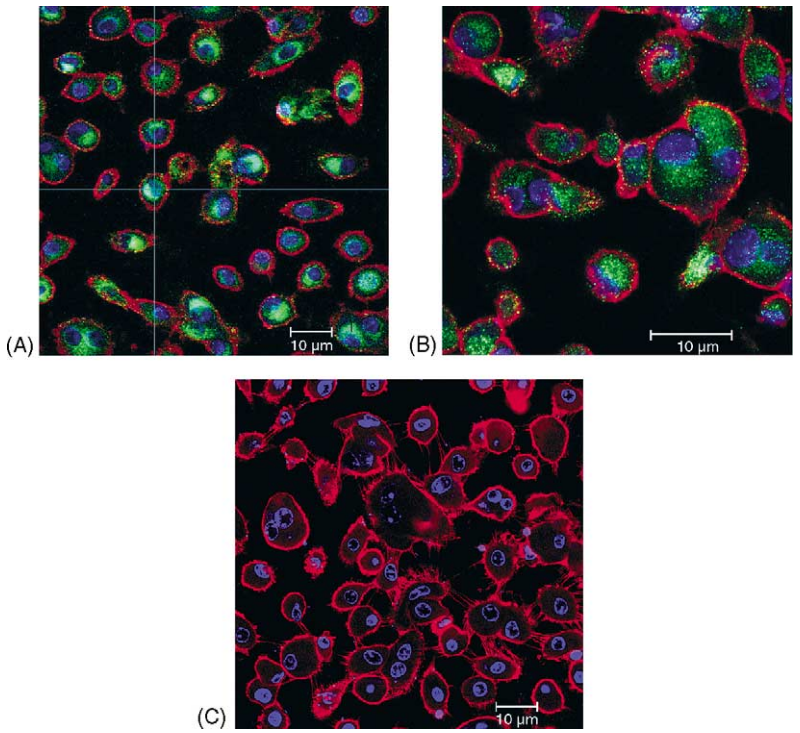

Fig. 8. Cellular uptake and intracellular distribution of HSA nanoparticles. Autofluorescent HSA nanoparticles (green) were incubated at a concentration of 25 µg/ml with primary human macrophages for 3 h and visualized by confocal microscope imaging using 63× magnification, 1× electronic zoom (A and C) and 63× magnification, 2× electronic zoom (B). Cell nuclei were stained with TOTO-3-iodid (blue) and cell membranes were stained with TRITC-conjugated concanavalin A (red). Primary human macrophages without incubation of HSA nanoparticles are shown in (C).

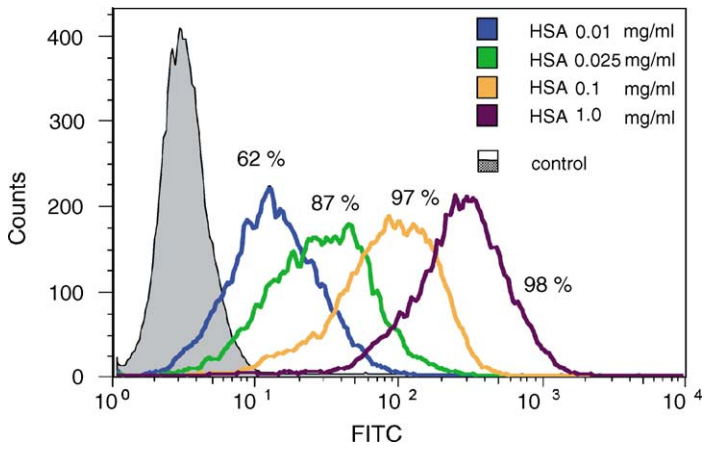

Fig. 9. FACS profile of primary human macrophages incubated with different concentrations of HSA nanoparticles. Cellular uptake of autofluorescent HSA nanoparticles was quantified acquiring fluorescence of the cells in the FITC channel. Percentage of cells with internalized HSA nanoparticles is indicated by the number above each graph. Control cells without HSA nanoparticles are indicated by the solid grey pattern.

diameter and −44 mV surface charge could serve as drug delivery systems in future applications into cells of the mononuclear phagocyte system.

4. Conclusion

The present study shows that HSA nanoparticles can be prepared with predictable and reproducible size, in a size range between 150 and 280 nm, by an aqueous desolvation process. Adjustment of the pH value in the presence of sodium chloride prior to the protein desolvation and particle purification by repeated (alkaline) washing represent the basic improvements in the preparation procedure. The pH value as well as the buffer concentration in a HSA nanoparticle suspension were identified as crucial parameters for particle stability. HSA nanoparticles proofed to be taken up into primary human macrophages into non-nucleic intracellular compartments. In combination with our previous work on the covalent surface modification of protein-based nanoparticles the present study represents a further step towards a rational colloidal carrier design.

Acknowledgements

This work is supported by the German Bundesministerium für Bildung und Forschung (Project 03C0308A and 03C0308C).

References

Carter, D.C., Ho, J.X., 1994. Structure of serum albumin. Adv. Protein Chem. 45, 153–203.

Gallo, J.M., Hung, C.T., Perrier, D.G., 1984. Analysis of albumin microsphere preparation. Int. J. Pharm. 22, 63–74.

Harashima, H., Sakata, K., Funato, K., Kiwada, H., 1994. Enhanced hepatic uptake of liposomes through complement activation depending on the size of liposomes. Pharm. Res. 11, 402–406.

Hirayama, K., Akashi, S., Furuya, M., Fukuhara, K., 1990. Rapid confirmation and revision of the primary structure of bovine serum albumin by ESIMS and Frit-FAB LC/MS. Biochem. Biophys. Res. Commun. 173, 639–646.

Langer, K., Coester, C., von Briesen, H., Kreuter, J., 2000. Preparation of avidin-labeled protein nanoparticles as carriers for biotinylated peptide nucleic acid (PNA). Eur. J. Pharm. Biopharm. 49, 303–307.

Lin, W., Coombes, A.G.A., Davies, M.C., Davis, S.S., Illum, L., 1993. Preparation of sub-100 nm human serum albumin nanospheres using a pH-coacervation method. J. Drug Target. 1, 237–243.

Marty, J.J., Oppenheimer, R.C., Speiser, P., 1978. Nanoparticles—a new colloidal drug delivery system. Pharm. Acta Helv. 53, 17–23.

Moghimi, S.M., Hunter, A.C., Murray, J.C., 2001. Long-circulating and target-specific nanoparticles: theory to practice. Pharmacol. Rev. 58, 283–318.

Müller, G.M., Leuenberger, H., Kissel, T., 1996. Albumin nanospheres as carriers for passive drug targeting: an optimized manufacturing technique. Pharm. Res. 13, 32–37.

Romero, E.L., Morilla, M.J., Regts, J., Koning, G.A., Scherphof, G.L., 1999. On the mechanism of hepatic transendothelial passage of large liposomes. FEBS Lett. 448, 193–196.

Schuck, P., 2000. Size distribution analysis of macromolecules by sedimentation velocity ultracentrifugation and Lamm equation modeling. Biophys. J. 78, 1606–1619.

Schuck, P., Rossmanith, P., 2000. Determination of the sedimentation coefficient distribution by least-squares boundary modeling. Biopolymers 54, 328–341.

Schuck, P., Perugini, M.A., Gonzales, N.R., Howlett, G.J., Schubert, D., 2002. Size-distribution analysis of proteins by analytical ultracentrifugation: strategies and application to model systems. Biophys. J. 82, 1096–1111.

Smith, P.K., Krohn, R.I., Hermanson, G.T., Mallia, A.K., Gartner, F.H., Provenzano, M.D., Fujimoto, E.K., Goeke, N.M., Olson, B.J., Klenk, D.C., 1985. Measurement of protein using bicinchoninic acid. Anal. Biochem. 150, 76–85.

Vogel, V., Langer, K., Balthasar, S., Schuck, P., Mächtle, W., Haase, W., van den Broek, J.A., Tziatzios, C., Schubert, D., 2002. Characterization of serum albumin nanoparticles by sedimentation velocity analysis and electron microscopy. Prog. Colloid Polym. Sci. 119, 31–36.

Weber, C., Kreuter, J., Langer, K., 2000a. Preparation of surface modified protein nanoparticles by introduction of sulfhydryl groups. Int. J. Pharm. 211, 67–78.

Weber, C., Coester, C., Kreuter, J., Langer, K., 2000b. Desolvation process and surface characteristics of protein nanoparticles. Int. J. Pharm. 194, 91–102.

Westcott, C.C., 1978. pH Measurements. Academic Press, New York, pp. 123–130.